

Original Article

Cite this article: Ling J, Li P, Yuan C, and Tserendash N. Decoupling between Nd-Hf isotopic evolution of Permian to Triassic granitoids and crustal thickness variation in the westernmost Mongol-Okhotsk Orogen. *Geological Magazine* 162(e16): 1–9. <https://doi.org/10.1017/S0016756825000081>

Received: 17 October 2024

Revised: 27 February 2025

Accepted: 17 April 2025


Keywords:

Mongol-Okhotsk Orogen; Hangay Mountains; Nd-Hf isotopes; La_N/Yb_N ratio; crustal thickness

Corresponding author:

Pengfei Li; Emails: pengfeili@gig.ac.cn; pengfeili2013@gmail.com

Decoupling between Nd-Hf isotopic evolution of Permian to Triassic granitoids and crustal thickness variation in the westernmost Mongol-Okhotsk Orogen

Jiaqi Ling^{1,2} , Pengfei Li^{1,2}, Chao Yuan^{1,2} and Narantsetseg Tserendash³

¹State Key Laboratory of Deep Earth Processes and Resources, Guangzhou Institute of Geochemistry, Chinese Academy of Sciences, Guangzhou, China; ²University of Chinese Academy of Sciences, Beijing, China and ³Institute of Geology, Mongolian Academy of Sciences, Ulaanbaatar, Mongolia

Abstract

Nd-Hf isotope evolution in arc magmas has been widely used to trace the advance and retreat of subduction zones over time. However, the reliability of this method has been questioned. One way to assess its validity is by comparing it with La_N/Yb_N or Sr/Yb ratios, which are well-established proxies for crustal thickness. In this study, we present new Nd-Hf isotopic data from the Permian to Triassic Hangay Batholith in the western Mongol-Okhotsk Orogen (Hangay Mountains), to evaluate the role of Nd-Hf isotopes in tracing crustal thickness variations along convergent plate boundaries. Our results show that granitoids from the Hangay Batholith likely originated from partial melting of crustal materials, with a possible mantle contribution. These granitoids have moderate $\epsilon_{Nd}(t)$ and $\epsilon_{Hf}(t)$ values, with no significant shift from Permian to Triassic, which contrasts with the continuous crustal thickening indicated by La_N/Yb_N ratios. This inconsistency between Nd-Hf isotope evolution and crustal thickness variation is likely due to the heterogeneous crustal architecture in this accretionary orogen. Our findings highlight the need for caution when linking Hf and Nd isotope evolution with extensional and contractional tectonics.

1. Introduction

Tracing crustal thickness through deep time is key to understanding orogenic evolution, as the thickness of the overriding plate is sensitive to tectonic transitions, such as shifts between trench retreat and advance along convergent plate boundaries (Luffi & Ducea, 2022; Profeta *et al.* 2015; Sundell *et al.* 2022; Tang *et al.* 2020; Zhu *et al.* 2017). Recently, several proxies based on trace elements in arc magmas, such as La_N/Yb_N and Sr/Y ratios, have been proposed to estimate crustal thickness. These proxies are based on the assumption that thicker arc crust generally shows higher La_N/Yb_N or Sr/Y ratios, due to the fractionation of garnet and/or amphibole during magma differentiation in deeper crustal environments (Chapman *et al.* 2015; Luffi & Ducea, 2022; Profeta *et al.* 2015; Zhu *et al.* 2017). These methods have been successfully applied to reconstruct crustal thickness in both modern and ancient orogens, such as Tibet and the central Andes (Profeta *et al.* 2015; Zhu *et al.* 2017). Alternatively, Nd-Hf isotope evolution in arc magmas has also been used to trace subduction dynamics (such as the advance and retreat of subduction zones) in regions like eastern Australia and Central Asia given that crustal thickening can lead to increased crustal input into the magma, and episodes of crustal extension typically result in a greater contribution of mantle-derived juvenile materials to the magma (Collins *et al.* 2011; Han *et al.* 2016; Kemp *et al.* 2009; Li *et al.* 2019; Zhang *et al.* 2016). However, the time-shifted Hf and Nd isotope evolution observed in the Sierra Nevada batholith of the Cordilleran orogen has been linked to variable contributions of fertile materials to the magma, driven by cyclical changes in lithosphere fertility and foundering, rather than trench migration (Chapman & Ducea, 2019). A recent study of the Patagonian Andes suggests a potential decoupling between isotopic trends and tectonic transitions (Rey *et al.* 2024), challenging the use of isotopic records to track tectonic shifts. This apparent discrepancy between trace element and isotope proxies in tracking crustal thickness can be further evaluated by comparing La_N/Yb_N trends with Nd-Hf isotope evolution in the same region.

In this study, we investigate the westernmost Mongol-Okhotsk Orogen (Hangay Mountains) to evaluate the reliability of Nd-Hf isotopes in tracing variations in crustal thickness. Our results reveal a decoupling between the Nd-Hf isotopic evolution of the Permian–Triassic Hangay Batholith and changes in crustal thickness, highlighting the limitations of using isotopic records to track transitions between extensional and contractional tectonic regimes.

© The Author(s), 2025. Published by Cambridge University Press. This is an Open Access article, distributed under the terms of the Creative Commons Attribution licence (<https://creativecommons.org/licenses/by/4.0/>), which permits unrestricted re-use, distribution and reproduction, provided the original article is properly cited.



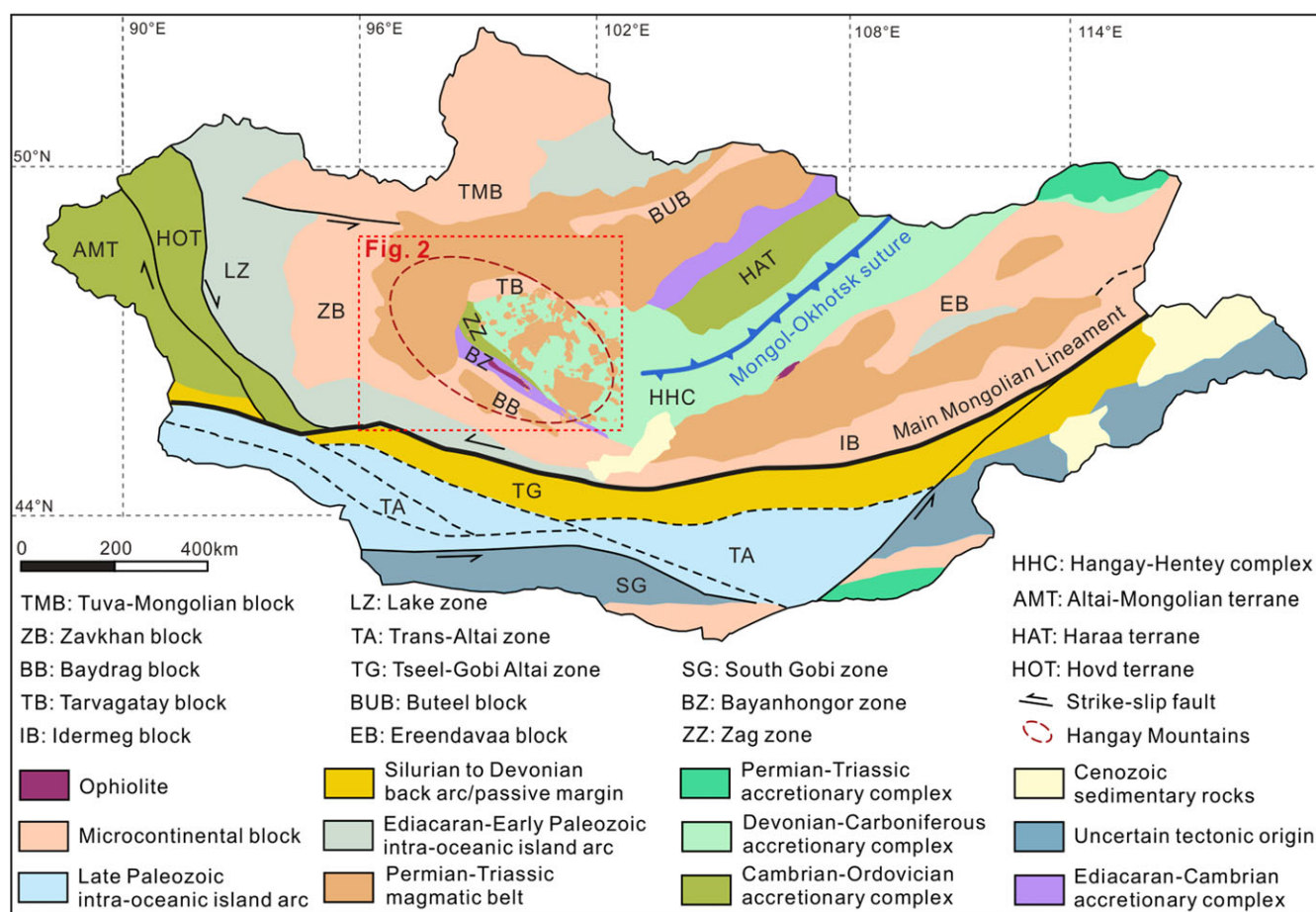


Figure 1. The tectonic map of Mongolia, which is modified from Li *et al.* (2022) and Ling *et al.* (2024).

2. Geological setting

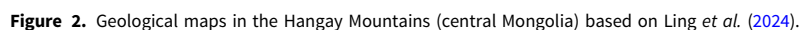
The Mongol-Okhotsk Orogen extends from the Hangay Mountains (central Mongolia) to the Okhotsk Sea (Fig. 1). It shows a U-shaped geometry in a map view, which was referred to as the Mongolian Orocline or the Tuva-Mongolian Orocline (Li *et al.* 2022; Van der Voo *et al.* 2015; Xiao *et al.* 2015). Precambrian microcontinental blocks, Late Neoproterozoic to Palaeozoic accretionary complexes, and Permian to Jurassic magmatism in the Mongol-Okhotsk Orogen are spatially distributed around the Mongolian Orocline (Fig. 1). In the Early Permian, an Andean-type subduction system was established around the whole Mongolian Orocline (Badarch *et al.* 2002; Donskaya *et al.* 2013; Wang *et al.* 2022). This subduction system was likely terminated in the Jurassic as the development of the Mongolian orocline and the closure of the Mongol-Okhotsk Ocean (Van der Voo *et al.* 2015; Zhao *et al.* 2023).

Precambrian microcontinental blocks around the Hangay Mountains include the Tavragatay, Zavkhan, and Baydrag blocks (Figs. 1 and 2). The Tavragatay block in the north is dominated by Archaean to Palaeoproterozoic gneiss, amphibolite, and schist, which are overlain by Neoproterozoic to Early Cambrian limestone and Devonian-Carboniferous sandstone and conglomerate (Badarch *et al.* 2002; Kozakov *et al.* 2011; Kröner *et al.* 2014). Farther southwest, the Zavkhan block has a Proterozoic basement (Bold *et al.* 2016; Kröner *et al.* 2014), which is covered by Neoproterozoic volcanic rocks, clastic rocks, and carbonates

(Kozakov *et al.* 2015; Kröner *et al.* 2014). In the south, the Baydrag block comprises Archaean to Proterozoic tonalitic to granitic gneiss and granulite, overlain by Neoproterozoic sandstone and Devonian to Permian volcanoclastic rocks (Demoux *et al.* 2009; Kröner *et al.* 2017).

Late Neoproterozoic to Palaeozoic accretionary complexes were developed around the Hangay Mountains, which include, from west to east, the Bayanhongor zone, the Zag zone, and the Hangay-Hentey complex (Fig. 2) (Şengör *et al.* 2018; Şengör *et al.* 1993). The Bayanhongor zone is represented by a pile of late Neoproterozoic to Cambrian tectonic mélange with ~647–630 Ma ophiolite incorporated (Buchan *et al.* 2001; Jian *et al.* 2010). The Zag zone mainly consists of Cambrian to Ordovician pelitic and psammitic schist, metasilstone, metasandstone, and minor conglomerate that were metamorphosed under greenschist facies (Badarch *et al.* 2002; Buchan *et al.* 2001; Li *et al.* 2022; Osozawa *et al.* 2008). The Hangay-Hentey complex predominantly consists of the Devonian to Carboniferous turbidite that is mixed with the exotic oceanic plate stratigraphy of interlayered basalt and chert (Erdenesaihan *et al.* 2013a; Tsukada *et al.* 2013).

Both Precambrian microcontinental blocks and accretionary complexes around the Hangay Mountains are intruded by Permian-Triassic magmatic rocks (Hangay Batholith) that represent a magmatic arc associated with the subduction of the Mongol-Okhotsk oceanic plate (Figs. 1 and 2) (Badarch *et al.* 2002; Donskaya *et al.* 2013; Ling *et al.* 2024; Wang *et al.* 2022).



Whole-rock Sr and Nd isotopes were analysed by Neptune Plus MC-ICP-MS (Thermo Fisher Scientific, Dreieich, Germany) at the Wuhan Sample Solution Analytical Technology Co., Ltd, Wuhan,

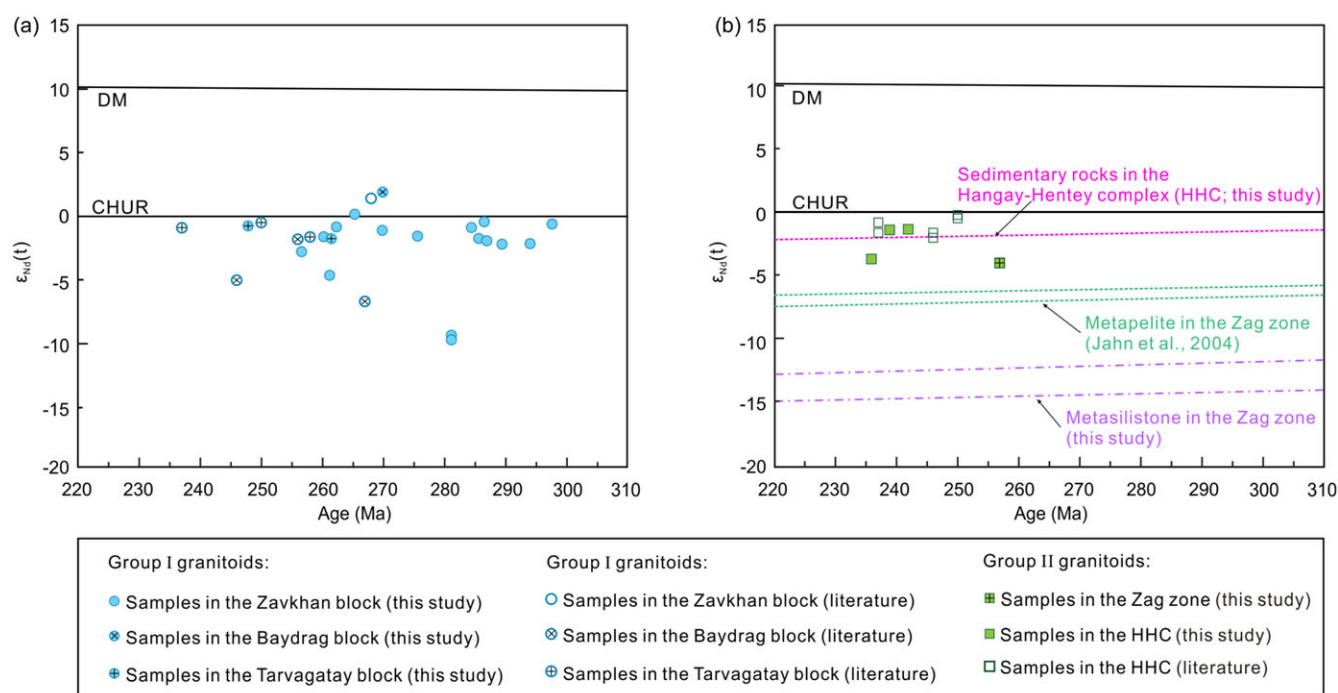


Figure 3. (a) Diagram of $\epsilon_{Nd}(t)$ values versus crystallizing ages for Group I granitoids; (b) diagram of $\epsilon_{Nd}(t)$ values versus crystallizing ages for Group II granitoids and sedimentary rocks in the Zag zone and the Hangay-Hentey complex. The Nd isotopic data in the literature are from Jahn *et al.* (2004) and Yarmolyuk *et al.* (2016).

China. Approximately 50–100 mg of powdered sample was placed in a Teflon bomb, and 1–3 ml of HNO_3 and HF were gradually added. Afterward, the Teflon bomb was put in an oven, and heated to 190°C over 24 h. After cooling, the Teflon bombs were evaporated to dryness, and then 1 ml of HNO_3 was added and evaporated to dryness again. Next, 1.5 ml of HCl was added to the evaporated sample. Following this, the sample was processed by centrifuge, with Sr fractions separated with an ion-exchange column of AG50W resin. Nd fractions were further separated by ion-exchange columns of LN resins. Finally, Sr and Nd isotopes were collected for mass-spectrometric measurement.

In this study, the Sr isotopic standard of NBS SRM 987 was applied to estimate instrumental reproducibility and accuracy. The measured $^{87}\text{Sr}/^{86}\text{Sr}$ ratio of the NBS SRM 987 is 0.710243 ± 5 (2σ , $n = 14$), consistent with the reported value (0.710241 ± 12 ; Thirlwall, 1991). In addition, two Nd isotopic standards (Jndi-1 and GSB) were applied to evaluate the instrumental reproducibility and accuracy during the analysis of the samples. The $^{143}\text{Nd}/^{144}\text{Nd}$ ratio of the Jndi-1 is 0.512116 ± 9 (2σ , $n = 7$), which is similar to the recommended values (0.512115 ± 7 , Tanaka *et al.* 2000). The measured $^{143}\text{Nd}/^{144}\text{Nd}$ ratio of the GSB is 0.512440 ± 5 (2σ , $n = 9$), compatible with the recommended values (0.512439 ± 10 ; Li *et al.* 2017).

3.b.2. Zircon Hf isotope

Zircon Hf isotope was analysed by the Neptune Plus MC-ICP-MS (Thermo Scientific) at the Key Laboratory of Mineralogy and Metallogeny (Guangzhou Institute of Geochemistry, Chinese Academy of Sciences) connected with a RESOLUTION M-50 193 nm laser ablation system (Resonetics). The diameter and frequency of the laser were set to 45 μm and 6 Hz, respectively. The laser energy density of 4 Jcm^{-2} was applied to ablate zircons. Helium was used as the carrier gas to transport ablating materials. ^{173}Yb and

^{175}Lu were used for correcting the isobaric interference of ^{176}Yb and ^{176}Lu on ^{176}Hf . The recommended values of $^{176}\text{Yb}/^{173}\text{Yb}$ and $^{176}\text{Lu}/^{175}\text{Lu}$ adapted for the correction are 0.79381 (Segal *et al.* 2003) and 0.02656 (Wu *et al.* 2006), respectively. The detailed analytical method and data reduction are documented in Wu *et al.* (2006) and Li *et al.* (2015). In this study, the chondritic values of $^{176}\text{Hf}/^{177}\text{Hf}$ (0.282772) and $^{176}\text{Lu}/^{177}\text{Hf}$ (0.0332), reported by Blichert-Toft & Albarede (1997), were adapted to calculate the $\epsilon_{Hf}(t)$ values. The present-day depleted mantle values ($^{176}\text{Hf}/^{177}\text{Hf} = 0.283250$ and $^{176}\text{Lu}/^{177}\text{Hf} = 0.0384$, Griffin *et al.* 2000) were taken to calculate the single-stage Hf model ages (T_{DM1}). Two-stage model ages (T_{DM2}) were calculated by using the mean $f_{Lu/Hf}$ value of -0.34 for the lower crust (Amelin *et al.* 1999) and 0.16 for the depleted mantle (Griffin *et al.* 2002).

4. Results

Whole-rock Sr-Nd and zircon Hf isotopic data of granitoids from the Hangay Batholith are listed in Tables S2 and S3. Spatially, Group I granitoids were emplaced into the Precambrian basement terranes, and Group II mainly intruded into accretionary complexes (Fig. 2), but both of them have similar Sr-Nd-Hf isotopic composition as documented below.

Eighteen samples of Group I granitoids with Permian ages are characterized by initial $^{87}\text{Sr}/^{86}\text{Sr}$ ratios from 0.70449 to 0.71117, and their $\epsilon_{Nd}(t)$ values range from -9.6 to $+1.7$ with two-stage Nd model ages of 0.9–1.8 Ga (Fig. 3a). These samples have a wide range of zircon Hf isotopes ($\epsilon_{Hf}(t) = -5.4$ to $+12.6$), which correspond to two-stage Hf model ages from 0.5 Ga to 1.6 Ga (Fig. 4a). The other sample of Group I granitoids has a Triassic age (~ 248 Ma), with an initial $^{87}\text{Sr}/^{86}\text{Sr}$ ratio of 0.70541 and a $\epsilon_{Nd}(t)$ value is -0.7 (Fig. 3a). This sample has $\epsilon_{Hf}(t)$ values between $+1.2$ and $+9.5$, which correspond to two-stage Hf model ages of (0.7–1.2 Ga, Fig. 4a).

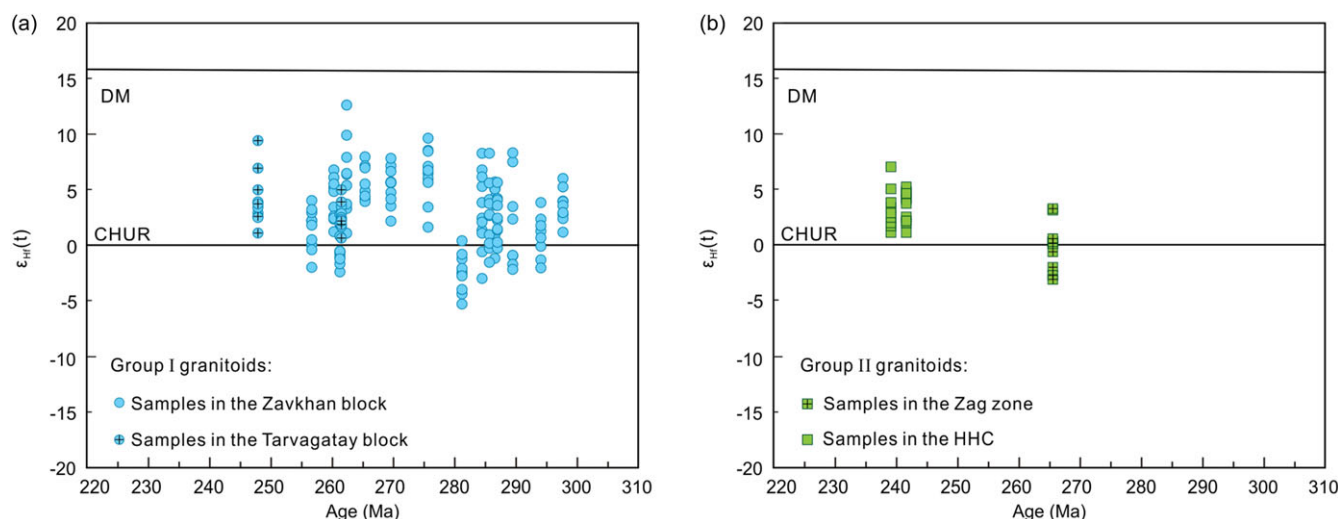


Figure 4. (a) Diagram of $\epsilon_{\text{Hf}}(t)$ values versus crystallizing ages for Group I granitoids; (b) diagram of $\epsilon_{\text{Hf}}(t)$ values versus crystallizing ages for Group II granitoids.

One Permian sample (~257 Ma) of Group II granitoids has a low initial $^{87}\text{Sr}/^{86}\text{Sr}$ ratio of 0.70612, and a $\epsilon_{\text{Nd}}(t)$ value of -4.2 (Fig. 3b). This sample shows a wide $\epsilon_{\text{Hf}}(t)$ values (-3.2 to $+3.2$) and two-stage Hf model ages (1.1–1.5 Ga; Fig. 4b). The other four samples of Group II granitoids yield Triassic ages, with low initial $^{87}\text{Sr}/^{86}\text{Sr}$ ratios (0.70508–0.70712) and moderate $\epsilon_{\text{Nd}}(t)$ values from -1.5 to -3.8 (corresponding to two-stage Nd model age of 1.1–1.3 Ga; Fig. 3b). Two of them were analysed for the Hf isotope, giving positive $\epsilon_{\text{Hf}}(t)$ values ($+1.1$ to $+7.0$) that correspond to two-stage Hf model ages from 0.8 Ga to 1.2 Ga (Fig. 4b).

Whole-rock Sr-Nd isotopic data for four samples of sedimentary rocks from Palaeozoic accretionary complexes are summarized in Table S2. Two metasiltsstones (L19M24 and L19M57) are from the Cambrian to Ordovician Zag Zone (Fig. 2). Assuming ~460 Ma deposition ages for these two samples, we obtain initial $^{87}\text{Sr}/^{86}\text{Sr}$ ratios of 0.71444 and 0.72544, as well as $\epsilon_{\text{Nd}}(t)$ values of -10.6 and -12.8 (corresponding to two-stage Nd model ages of 2.0 Ga and 2.2 Ga, respectively) for the two metasiltsstone samples (Table S2). The other two samples (L19M18-3 and L19M89-5) from the Devonian to Carboniferous Hangay-Hentey Complex give low initial $^{87}\text{Sr}/^{86}\text{Sr}$ ratios (0.70545 and 0.70580) and moderate $\epsilon_{\text{Nd}}(t)$ values of -1.2 and $+0.7$ (Table S2), based on an assumption of their deposition ages at ~350 Ma.

5. Discussion

5.a. Petrogenesis

Previous studies show that the Hangay Batholith likely represents a magmatic arc associated with the subduction of the Mongol-Okhotsk Ocean based on rock associations and their geochemical characteristics (Donskaya *et al.* 2013; Wang *et al.* 2022). Granitoids from the Hangay Batholith have lower Cr and Ni contents than mantle-derived primary melts (Ni >400 ppm and Cr >1000 ppm; Şengör *et al.* 1993; Wilson, 1989), suggesting a potential crustal source (Donskaya *et al.* 2013; Jahn *et al.* 2004; Ling *et al.* 2024; Wang *et al.* 2022; Yarmolyuk *et al.* 2016). They are enriched in LILEs and depleted in HFSEs, which is compatible with the composition of continental crust (Donskaya *et al.*, 2013; Jahn *et al.* 2004; Ling *et al.* 2024; Rudnick & Gao, 2003; Wang *et al.* 2022; Yarmolyuk *et al.* 2016).

Group I granitoids were emplaced into Precambrian microcontinental blocks of Tarvagatay, Zavkhan, and Baydrag (Fig. 2), which are characterized by a wide range of $\epsilon_{\text{Nd}}(t)$ and $\epsilon_{\text{Hf}}(t)$ values for their basement rocks (Fig. 5a and b). Nd and Hf isotopic data for Group I granitoids from both this study and previous work (Jahn *et al.* 2004; Yarmolyuk *et al.* 2016) are plotted either above or on the evolution lines of Precambrian microcontinental blocks (Fig. 5a and b). In the Sr-Nd diagram, Group I granitoids fall near the mixing curve of Precambrian microcontinental blocks and depleted mantle (DM) (Fig. 5c), indicating that they are likely sourced from the melting of the Precambrian microcontinental blocks with additional mantle contribution that is also supported by the occurrence of mafic microgranular enclaves within some Group I granitoids (Fig. S1e and f).

Group II granitoids intruded into the Palaeozoic accretionary complex of the Zag zone and the Hangay-Hentey complex (Fig. 2). One Permian sample (~257 Ma) within the Zag zone exhibits moderate $\epsilon_{\text{Hf}}(t)$ and $\epsilon_{\text{Nd}}(t)$ values (Fig. 5a and b). The $\epsilon_{\text{Nd}}(t)$ value is slightly elevated above the evolution lines of the Zag zone (Fig. 5a), suggesting a minor mantle contribution to the magma source. This is further supported by the mixing curve between metasiltsstones in the Zag zone and depleted mantle (DM) in the Sr-Nd diagram, where the Permian sample is plotted near this mixing curve (Fig. 5d). The rest of the Triassic granitoids that intruded into the Hangay-Hentey complex have a roughly similar Sr-Nd isotopic composition as the Hangay-Hentey complex (Fig. 5a and d), suggesting that these granitoids may predominantly originate from the melting of Hangay-Hentey complex though the possible minor contribution of the adjacent Zag zone cannot be excluded.

5.b. Decoupling between isotopic evolution and crustal thickness variation

Our results show that both Group I and II granitoids of the Hangay Batholith are sourced from crustal melting with possible additional contribution of mantle materials. They have moderate $\epsilon_{\text{Nd}}(t)$ and $\epsilon_{\text{Hf}}(t)$ values without obvious increasing and decreasing trend over time (Fig. 6b and c). Such an isotopic evolution trend seems indicative of a relatively constant crustal thickness of the westernmost Mongol-Okhotsk Orogen (around

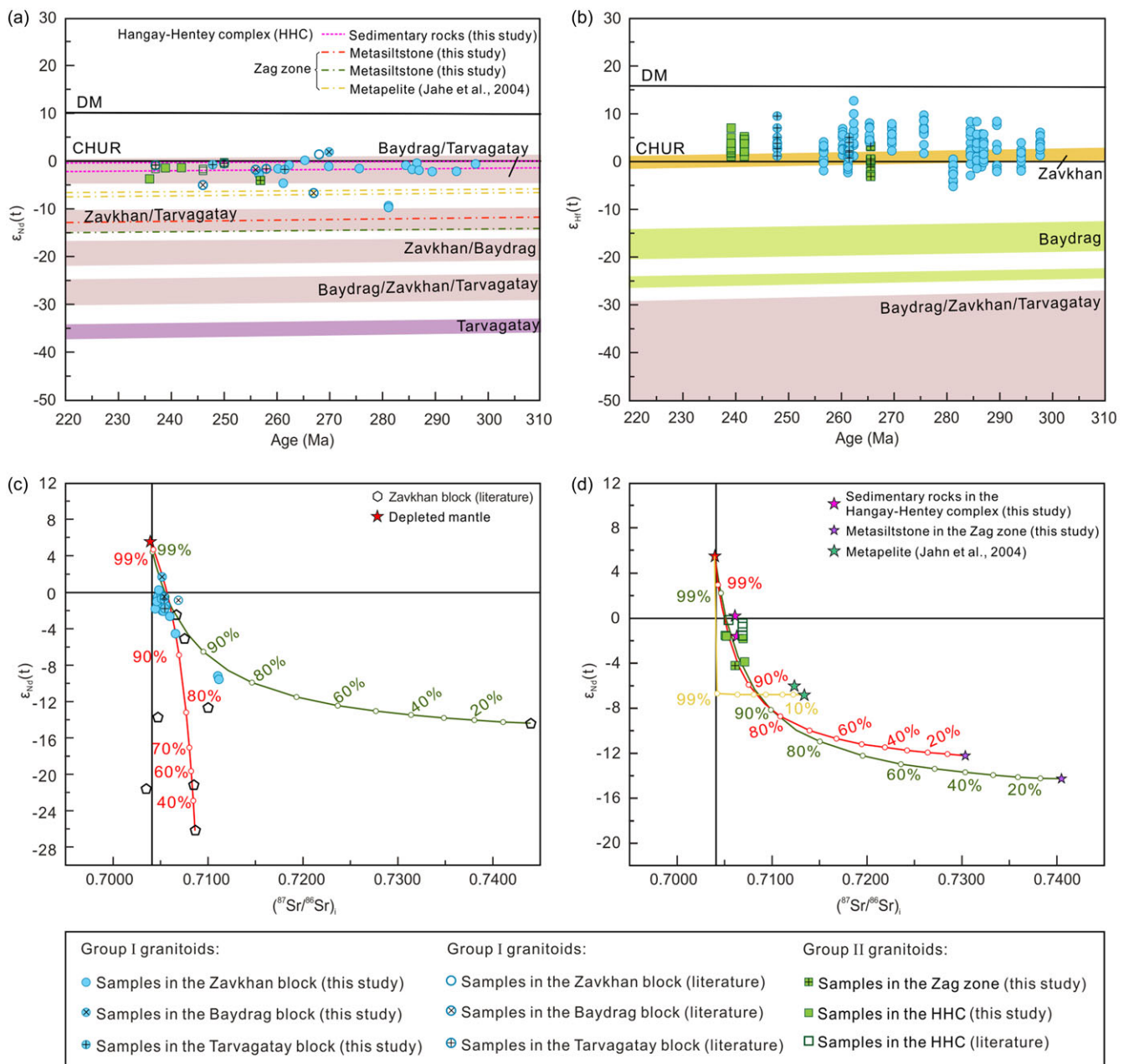


Figure 5. (a) Diagram of $\epsilon_{Nd}(t)$ versus crystallizing ages for granitoids from the Hangay Batholith; (b) diagram of $\epsilon_{Hf}(t)$ values versus crystallizing ages for the Hangay Batholith; (c) mixing $\epsilon_{Nd}(t)$ -initial $(^{87}Sr/^{86}Sr)_i$ curves between the depleted mantle and Precambrian blocks and their relationship with Group I granitoids (see details in the main text); (d) diagram of $\epsilon_{Nd}(t)$ values versus crystallizing ages, illustrating the potential relationship between Group II granitoids and accretionary complexes (see details in the main text). The isotopic data of the Precambrian blocks are from Kozakov *et al.* (2015); Kozakov *et al.* (2011); Kröner *et al.* (2017); Kröner *et al.* (2014) and Soejono *et al.* (2023), while Sr-Nd isotopic data of depleted mantle are from Salters and Stracke (2004).

Hangay Mountains) from Permian to Triassic. Previous studies from the Tasmanides (eastern Australia) and the western Central Asian Orogenic Belt show that a decreasing trend of $\epsilon_{Nd}(t)$ and $\epsilon_{Hf}(t)$ over time may illustrate an increasing contribution of crustal materials during magma generation and ascent, which could result from crustal thickening that causes more crustal inputs into magma (Collins *et al.* 2011; Han *et al.* 2016; Kemp *et al.* 2009). In contrast, an increasing trend of $\epsilon_{Nd}(t)$ and $\epsilon_{Hf}(t)$ over time implies the enhanced contribution of mantle-derived juvenile materials to magma, commonly in response to an episode of crustal extension (Collins *et al.* 2011; Han *et al.* 2016; Kemp *et al.* 2009; Li *et al.* 2019; Zhang *et al.* 2016).

Recent crustal thickness reconstruction in the westernmost Mongol-Okhotsk Orogen (around the Hangay Mountains) based on La_N/Yb_N ratios of granitoids from the Hangay Batholith suggests progressive crustal thickening from Permian to Triassic, with average crustal thickness increasing from ~50 km to ~65 km in response to inner-hinge contraction as progressive development of the Mongolian Orocline (Fig. 7a; Ling *et al.* 2024). This is inconsistent with the Hf and Nd isotopic evolution trend (Fig. 6b and c), which seems indicative of a constant crustal thickness as discussed above. The method for La_N/Yb_N ratio as a crustal thickness proxy is based on the theory that magmatic rocks originating from thicker arc crust generally possess higher La_N/Yb_N ratios than those in thinner arc crust given garnet

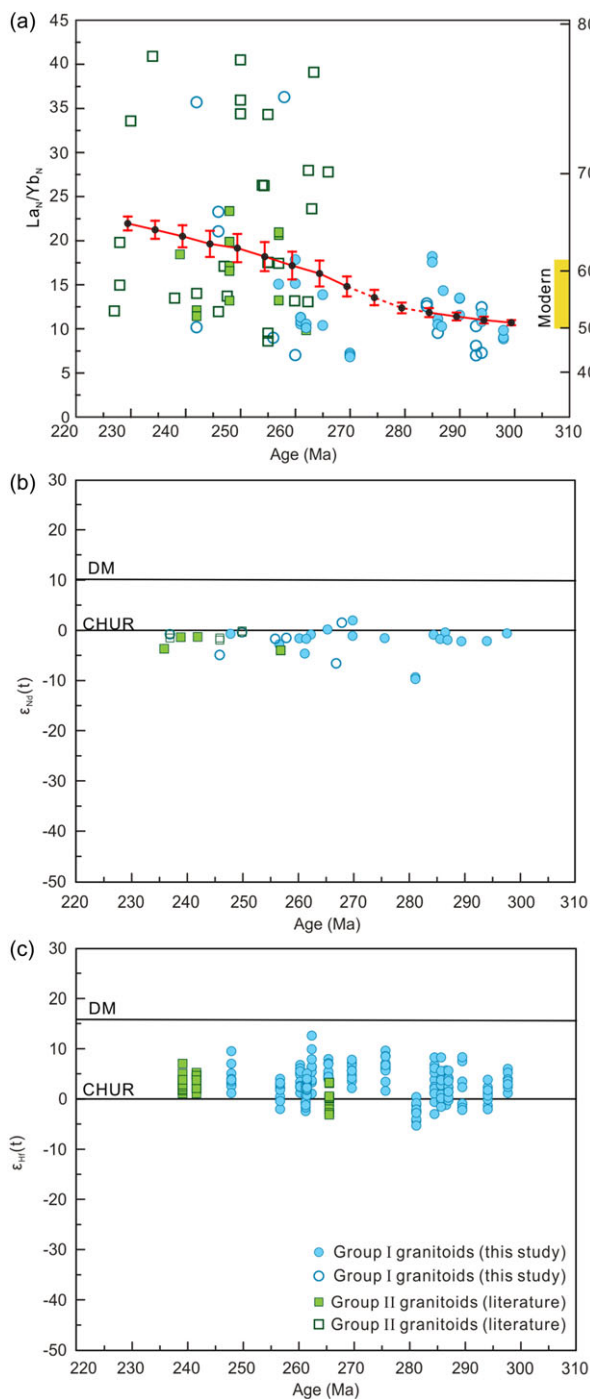


Figure 6. (a) Diagram of La_N/Yb_N ratios of granitoids versus ages from the Hangay Batholith, illustrating the increase in La_N/Yb_N ratios and crustal thickness from Permian to Triassic (modified from Ling *et al.*, 2024). The red line with two sigma error bars represents the average trend of La_N/Yb_N ratios as documented in Ling *et al.* (2024). The yellow rectangle shows the present-day crustal thickness around Hangay Mountains; (b) diagram of $\epsilon_{Nd}(t)$ versus crystallizing ages from the Hangay Batholith, showing no time-shifted trend; (c) diagram of $\epsilon_{Hf}(t)$ values versus crystallizing ages from the Hangay Batholith, indicating a relatively constant trend over time.

and/or amphibole fractionation during magma differentiation in a deeper crustal environment (Luffi & Ducea, 2022; Profeta *et al.* 2015). This method for tracing crustal thickness has been shown to be effective in both modern and ancient orogens (Luffi & Ducea, 2022; Profeta *et al.* 2015; Song *et al.* 2023; Wang *et al.* 2020; Zhu *et al.* 2017).

In contrast, the link between Hf and Nd isotopic evolution and crustal thickness variation is based on an assumption of relatively homogeneous composition for arc crust. However, the composition of the overriding plate along convergent plate boundaries could be heterogeneous or modified due to prolonged subduction, which is obvious in particular for the accretionary orogen, such as the Central Asian Orogenic Belt (Broussole *et al.* 2020). In the case of the westernmost Mongol-Okhotsk Orogen, the subduction might have initiated in the Ediacaran (Demoux *et al.* 2009; Jahn *et al.* 2004; Zhang *et al.* 2015), and lasted until the Early Mesozoic (Donskaya *et al.* 2013; Ling *et al.* 2021; Van der Voo *et al.* 2015; Wang *et al.* 2022). The prolonged subduction could result in the continuing addition of juvenile crust under the Precambrian microcontinents of Tarvagatay, Zavkhan, and Baydrag blocks via either magmatically underplating or tectonic accretion (Collins *et al.* 2011). In addition, Triassic Group II granitoids of the Hangay Batholith intruded into the Palaeozoic accretionary complexes of the Zag zone and the Hangay-Hentey complex, which are characterized by heterogeneous rock associations with overriding plate-derived sedimentary rocks (moderate $\epsilon_{Nd}(t)$ values as shown in Fig. 5a), mixed with off-scraping oceanic plate stratigraphy (basalt and chert) (Erdenesaihan *et al.* 2013b; Tsukada *et al.* 2013). Overall, it seems reasonable to propose a heterogeneous source for the Hangay Batholith. Consequently, the evolution of Hf and Nd isotopes does not appear to be sensitive to increases in crustal thickness, as the greater contribution of the relatively juvenile crust during progressive thickening would not significantly lower the $\epsilon_{Nd}(t)$ and $\epsilon_{Hf}(t)$ values.

Our results highlight a decoupling between the Permian to Triassic evolution of Hf and Nd isotopes in arc magmas and crustal thickness variation in the westernmost Mongol-Okhotsk Orogen. This decoupling may also occur in other arc systems over deep time. Therefore, caution is needed when linking Hf and Nd isotope evolution to crustal thickness variations, even though such links have commonly been used to trace subduction advance and retreat along convergent plate boundaries (Han *et al.* 2016; Kemp *et al.* 2009). A recent study in the Patagonian Andes shows a trend towards isotopically positive values as the back-arc extension related to the trench retreat, but it does not exhibit the trend towards isotopically negative values during the back-arc closure and arc-continent collision that is typically expected in advancing orogens (Rey *et al.* 2024). The prolonged juvenile isotopic signature for tens of millions of years after the back-arc basin closure in the Patagonian Andes has been attributed to the partial melting of underthrust isotopically juvenile crust that was formed during earlier back-arc extension (Rey *et al.* 2024), thus underscoring the limitations of using isotopic records to trace contractional and extensional tectonic processes.

6. Conclusions

This study obtains new whole-rock Sr-Nd and zircon Hf isotopic from granitoids of the Permian to Triassic Hangay Batholith and Palaeozoic accretionary complex in the westernmost Mongol-Okhotsk Orogen (Hangay Mountains). Group I granitoids of the Hangay Batholith, which intruded the Precambrian microcontinents, have predominantly moderate initial $^{87}Sr/^{86}Sr$ ratios (0.70449 to 0.71117), $\epsilon_{Nd}(t)$ values (−9.6 to +1.7) and zircon $\epsilon_{Hf}(t)$ values (−5.4 to +12.6). Similarly, Group II granitoids of the Hangay Batholith, which mainly intruded into Palaeozoic accretionary complexes, have moderate initial $^{87}Sr/^{86}Sr$ ratios (0.70508 to 0.70712), $\epsilon_{Nd}(t)$ values (−4.2 to −1.5), and $\epsilon_{Hf}(t)$ values (−3.2 to +7.0). Combining with isotope data from Precambrian

microcontinents and Palaeozoic accretionary complexes, we conclude that both Group I and II granitoids were produced by partial melting of crustal materials (microcontinents or accretionary complexes) with possible additional mantle contribution. In addition, Group I and II granitoids do not show time-shifted evolution of $\epsilon_{\text{Nd}}(t)$ and $\epsilon_{\text{Hf}}(t)$ values, which is decoupled with the crustal thickness variation as traced by $\text{La}_\text{N}/\text{Yb}_\text{N}$ ratios of these granitoids. Such a decoupling is likely due to the heterogeneous crustal architecture.

Supplementary material. The supplementary material for this article can be found at <https://doi.org/10.1017/S0016756825000081>

Acknowledgements. This study was financially supported by the National Science Foundation of China (grant no. 42172237), the international partnership programme of the Chinese Academy of Sciences (CAS) (grant no. 132744KYSB20200001), and Guangdong Province of China (grant no. 2019QN01H101). This is a contribution of the Guangzhou Institute of Geochemistry (GIG)-CAS (No. IS-3652).

Competing interests. The authors declare none.

References

- Amelin Y, Lee D-C, Halliday AN and Pidgeon RT (1999) Nature of the Earth's earliest crust from hafnium isotopes in single detrital zircons. *Nature* **399**, 252–55.
- Badarch G, Cunningham WD and Windley BF (2002) A new terrane subdivision for Mongolia: implications for the Phanerozoic crustal growth of Central Asia. *Journal of Asian Earth Sciences* **21**, 87–110.
- Blichert-Toft J and Albarede F (1997) The Lu-Hf geochemistry of chondrites and the evolution of the mantle-crust system. *Earth and Planetary Science Letters* **148**, 243–53.
- Bold U, Crowley JL, Smith EF, Sambuu O and Macdonald FA (2016) Neoproterozoic to early Paleozoic tectonic evolution of the Zavkhan terrane of Mongolia: implications for continental growth in the Central Asian orogenic belt. *Lithosphere* **8**, 729–50.
- Broussole A, Jiang Y, Sun M, Yu Y, Wong J, Shu T and Xu K (2020) Constraints of zircon Hf isotopes on ancient crustal reworking in the Early Paleozoic Altai accretionary wedge, Central Asian Orogenic Belt. *Journal of Asian Earth Sciences* **203**, 104538.
- Buchan C, Cunningham D, Windley BF and Tomurhuu D (2001) Structural and lithological characteristics of the Bayankhongor Ophiolite Zone, Central Mongolia. *Journal of the Geological Society* **158**, 445–60.
- Chapman JB and Ducea MN (2019) The role of arc migration in Cordilleran orogenic cyclicity. *Geology* **47**, 627–31.
- Chapman JB, Ducea MN, DeCelles PG and Profeta L (2015) Tracking changes in crustal thickness during orogenic evolution with Sr/Y: an example from the North American Cordillera. *Geology* **43**, 919–22.
- Collins WJ, Belousova EA, Kemp AIS and Murphy JB (2011) Two contrasting Phanerozoic orogenic systems revealed by hafnium isotope data. *Nature Geoscience* **4**, 333–37.
- Demoux A, Kröner A, Badarch G and Jian P (2009) Zircon Ages from the Baydrag Block and the Bayankhongor Ophiolite Zone: time constraints on Late Neoproterozoic to Cambrian Subduction- and Accretion-Related Magmatism in Central Mongolia. *Journal of Geology* **117**, 377–97.
- Donskaya TV, Gladkochub DP, Mazukabzov AM and Ivanov AV (2013) Late Paleozoic-Mesozoic subduction-related magmatism at the southern margin of the Siberian continent and the 150 million-year history of the Mongol-Okhotsk Ocean. *Journal of Asian Earth Sciences* **62**, 79–97.
- Erdenesaihan G, Ishiwatari A, Orolmaa D, Arai S and Tamura A (2013a) Middle Paleozoic greenstones of the Hangay region, central Mongolia: remnants of an accreted oceanic plateau and forearc magmatism. *Journal of Mineralogical and Petrological Sciences* **108**, 303–25.
- Erdenesaihan G, Ishiwatari A, Orolmaa D, Arai S and Tamura A (2013b) Middle Paleozoic greenstones of the Hangay region, central Mongolia: remnants of an accreted oceanic plateau and forearc magmatism. *Journal of Mineralogical and Petrological Sciences* **108**, 303–25.
- Griffin WL, Pearson NJ, Elusive E, Jackson SE, van Achtenberg E, O'Reilly SY and She SR (2000) The Hf isotope composition of carbonic mantle: LAM-MC-ICPMS analysis of zircon megacrysts in kimberlites. *Geochimica et Cosmochimica Acta* **64**, 133–47.
- Griffin WL, Wang X, Jackson SE, Pearson NJ and O'Reilly SY (2002) Zircon geochemistry and magma mixing, SE China: in situ analysis of Hf isotopes, Tonglu and Pingtan igneous complexes. *Lithos* **61**, 237–69.
- Han Y, Zhao G, Cawood PA, Sun M, Eizenhöfer PR, Hou W, Zhang X and Liu Q (2016) Tarim and North China cratons linked to northern Gondwana through switching accretionary tectonics and collisional orogenesis. *Geology* **44**, 95–98.
- Jahn BM, Capdevila R, Liu D-Y, Vernon A and Badarch G (2004) Sources of Phanerozoic granitoids in the transect Bayanhongor–Ulaan Baatar, Mongolia: geochemical and Nd isotopic evidence, and implications for Phanerozoic crustal growth. *Journal of Asian Earth Sciences* **23**, 629–53.
- Jian P, Kröner A, Windley BF, Shi Y, Zhang F, Miao L, Tomurhuu D, Zhang W and Liu D (2010) Zircon ages of the Bayankhongor ophiolite mélange and associated rocks: time constraints on Neoproterozoic to Cambrian accretionary and collisional orogenesis in Central Mongolia. *Precambrian Research* **177**, 162–80.
- Kemp AIS, Hawkesworth CJ, Collins WJ, Gray CM and Blevin PL (2009) Isotopic evidence for rapid continental growth in an extensional accretionary orogen: the Tasmanides, eastern Australia. *Earth and Planetary Science Letters* **284**, 455–66.
- Kozakov IK, Kirnozova TI, Kovach VP, Terent'eva LB, Tolmacheva EV, Fugzan MM and Erdenezhargal C (2015) Late Riphean age of the crystalline basement of the carbonate cover of the Dzabkhan microcontinent. *Stratigraphy and Geological Correlation* **23**, 237–45.
- Kozakov IK, Kozlovsky AM, Yarmolyuk VV, Kovach VP, Bibikova EV, Kirnozova TI, Plotkina YV, Zagornaya NY, Fugzan MM, Erdenezhargal C, Lebedev VI and Eenjin G (2011) Crystalline complexes of the Tarbagatai block of the early caledonian superterrane of Central Asia. *Petrology* **19**, 426–44.
- Kröner A, Kovach VP, Kozakov IK, Aranovich L, Xie HQ, Tolmacheva E, Kirnozova T, Fugzan M, Serebryakov N, Wang KL and Lee HY (2017) Granulites and Palaeoproterozoic lower crust of the Baidarik Block, Central Asian Orogenic Belt of NW Mongolia. *Journal of Asian Earth Sciences* **145**, 393–407.
- Kröner A, Kovach VP, Kozakov IK, Kirnozova T, Azimov P, Wong J and Geng HY (2014) Zircon ages and Nd-Hf isotopes in UHT granulites of the iber complex: a cratonic terrane within the Central Asian Orogenic Belt in NW Mongolia. *Gondwana Research* **27**, 1392–406.
- Li D, He D, Qi X and Zhang N (2015) How was the Carboniferous Balkhash–West Junggar remnant ocean filled and closed? Insights from the Well Tacan-1 strata in the Tacheng Basin, NW China. *Gondwana Research* **27**, 342–62.
- Li J, Tang S-H, Zhu X-K and Pan C-X (2017) Production and certification of the reference material GSB 04-3258-2015 as a $^{143}\text{Nd}/^{144}\text{Nd}$ isotope ratio reference. *Geostandards and Geoanalytical Research* **41**, 255–62.
- Li P-F, Sun M, Narantsetseg T, Jourdan F, Hu W-W and Yuan C (2022) First structural observation around the hinge of the Mongolian Orocline (Central Asia): implications for the geodynamics of oroclinal bending and the evolution of the Mongol-Okhotsk Ocean. *Geological Society of America Bulletin* **134**, 1994–2006.
- Li P-F, Sun M, Shu C-T, Yuan C, Jiang YD, Zhang L and Cai KD (2019) Evolution of the Central Asian Orogenic Belt along the Siberian margin from Neoproterozoic-Early Paleozoic accretion to Devonian trench retreat and a comparison with Phanerozoic eastern Australia. *Earth-Science Reviews* **198**, 102951.
- Ling J-Q, Li P-F, Yuan C, Sun M, Zhang YY, Narantsetseg T, Wang XS, Jiang YD and Hu WW (2021) Ordovician to Devonian granitic plutons in the Hangay Range, Central Mongolia: petrogenesis and insights into the Paleozoic tectonic evolution of the westernmost Mongol-Okhotsk Orogen. *Lithos* **404–405**, 106463.
- Ling J, Li P, Yuan C, Rosenbaum G, Sun M, Li Z and Narantsetseg T (2024) The bending of a supra-subduction zone produced crustal thickening and arc

- migration of the Mongolian Orocline. *Communications Earth & Environment* **5**, 329.
- Luffi P and Ducea MN (2022) Chemical mohometry: assessing crustal thickness of ancient orogens using geochemical and isotopic data. *Reviews of Geophysics* **60**, e2021RG000753.
- Osozawa S, Tsolmon G, Majigsuren U, Sereenen J, Niitsuma S, Iwata N, Pavlis T and Jahn BM (2008) Structural evolution of the Bayanhongor region, west-central Mongolia. *Journal of Asian Earth Sciences* **33**, 337–52.
- Profeta L, Ducea MN, Chapman JB, Paterson SR, Gonzales SMH, Kirsch M, Petrescu L and DeCelles PG (2015) Quantifying crustal thickness over time in magmatic arcs. *Scientific Reports* **5**, 17786.
- Rey FM, Malkowski MA, Fosdick JC, Dobbs SC, Calderón M, Ghiglione MC and Graham SA (2024) Detrital isotopic record of a retreating accretionary orogen: an example from the Patagonian Andes. *Geology* **52**, 395–99.
- Rudnick RL and Gao S (2003) Composition of the continental crust. *Treatise on Geochemistry* **3**, 1–51.
- Salters VJM and Stracke A (2004) Composition of the depleted mantle. *Geochemistry, Geophysics, Geosystems* **5**, 1–27.
- Segal I, Halicz L and Platzner IT (2003) Accurate isotope ratio measurements of ytterbium by multiple collection inductively coupled plasma mass spectrometry applying erbium and hafnium in an improved double external normalization procedure. *Journal of Analytical Atomic Spectrometry* **18**, 1217–23.
- Şengör AMC, Natal'in BA, Sunal G and van der Voo R (2018) The tectonics of the altaids: crustal growth during the construction of the continental lithosphere of Central Asia between ~750 and ~130 Ma Ago. *Annual Review of Earth and Planetary Sciences* **46**, 439–94.
- Şengör AMC, Natal'in BA and Burtman VS (1993) Evolution of the Altaid tectonic collage and Palaeozoic crustal growth in Eurasia. *Nature* **364**, 299–307.
- Soejono I, Janoušek V, Peřestý V, Schulmann K, Svojtka M, Hanžl P, Hora JM, Míková J, Štípská P, Guy A, Collett S and Otgonbaatar D (2023) From Rodinian passive margin to peri-Siberian continental arc: evidence from the multiphase Neoproterozoic–early Paleozoic magmatic record of the Zavkhan Block in the Mongolian Collage. *Gondwana Research* **121**, 344–67.
- Song D, Mitchell RN, Xiao W, Mao Q, Wan B and Ao S (2023) Andean-type orogenic plateau as a trigger for aridification in the arcs of northeast Pangaea. *Communications Earth & Environment* **4**, 306.
- Sundell KE, George SWM, Carrapa B, Gehrels GE, Ducea MN, Saylor JE and Pepper M (2022) Crustal thickening of the northern central andean plateau inferred from trace elements in Zircon. *Geophysical Research Letters* **49**, e2021GL096443.
- Tanaka T, Togashi S, Kamioka H, Amakawa H, Kagami H and Hamamoto T (2000) Jndi-1: a neodymium isotopic reference in consistency with lajolla neodymium. *Chemical Geology* **168**, 279–81.
- Tang M, Ji W-Q, Chu X, Wu A and Chen C (2020) Reconstructing crustal thickness evolution from europium anomalies in detrital zircons. *Geology* **49**, 76–80.
- Thirlwall MF (1991) Long-term reproducibility of multicollector sr and nd isotope ratio analysis. *Chemical Geology* **94**, 85–104.
- Tsukada K, Nakane Y, Yamamoto K, Kurihara T, Otoh S, Kashiwagi K, Chuluun M, Gonchigdorj S, Nuramkhaan M, Niwa M and Tokiwa T (2013) Geological setting of basaltic rocks in an accretionary complex, Khangai-Khentei Belt, Mongolia. *Island Arc* **22**, 227–41.
- Van der Voo R, van Hinsbergen DJJ, Domeier M, Spakman W and Torsvik TH (2015) Latest Jurassic–earliest cretaceous closure of the Mongol-Okhotsk Ocean: a paleomagnetic and seismological-tomographic analysis. *Geological Society of America Special Paper* **513**, 589–606.
- Wang T, Tong Y, Xiao W-J, Guo L, Windley BF, Donskaya T, Li S, Tserendash N and Zhang JJ (2022) Rollback, scissor-like closure of the Mongol-Okhotsk Ocean and formation of an orocline: magmatic migration based on a large archive of age data. *National Science Review* **9**, nwab210.
- Wang X, Cai K, Sun M, Zhao G, Xiao W and Xia X (2020) Evolution of Late Paleozoic Magmatic Arc in the Yili Block, NW China: implications for oroclinal bending in the Western Central Asian Orogenic Belt. *Tectonics* **39**, 1–24.
- Wilson M (1989) *Igneous Petrogenesis*. London: Springer, Harper Collins Academic.
- Wu F-Y, Yang Y-H, Xie L-W, Yang J-H and Xu P (2006) Hf isotopic compositions of the standard zircons and baddeleyites used in U-Pb geochronology. *Chemical Geology* **234**, 105–26.
- Xiao W-J, Windley BF, Sun S, Li JL, Huang BC, Han CM, Yuan C, Sun M and Chen HL (2015) A tale of amalgamation of three Permo-Triassic collage systems in Central Asia: oroclines, sutures, and terminal accretion. *Annual Review of Earth and Planetary Sciences* **43**, 477–507.
- Yarmolyuk VV, Kozlovsky AM, Savatenkov VM, Kovach VP, Kozakov IK, Kotov AB, Lebedev VI and Eenjin G (2016) Composition, sources, and geodynamic nature of giant batholiths in Central Asia: evidence from the geochemistry and Nd isotopic characteristics of granitoids in the Khangai zonal magmatic area. *Petrology* **24**, 433–61.
- Zhang X, Zhao G, Sun M, Eizenhöfer PR, Han Y, Hou W, Liu D, Wang B, Liu Q and Xu B (2016) Tectonic evolution from subduction to arc-continent collision of the Junggar ocean: constraints from U-Pb dating and Hf isotopes of detrital zircons from the North Tianshan belt, NW China. *Geological Society of America Bulletin* **128**, 644–60.
- Zhang Y-Y, Sun M, Yuan C, Xu YG, Long XP, Tomurhuu D, Wang CY and He B (2015) Magma mixing origin for high Ba–Sr granitic pluton in the Bayankhongor area, central Mongolia: response to slab roll-back. *Journal of Asian Earth Sciences* **113**, 353–68.
- Zhao P, Xu B and Chen Y (2023) Evolution and final closure of the Mongol-Okhotsk Ocean. *Science China Earth Sciences* **66**, 2497–513.
- Zhu D-C, Wang Q, Cawood PA, Zhao ZD and Mo XX (2017) Raising the Gangdese mountains in southern tibet. *Journal of Geophysical Research: Solid Earth* **122**, 214–23.